Proceedings of the ASME 2012 International Design Engineering Technical Conferences &
Computers and Information in Engineering Conference
IDETC/CIE 2012
August 12-15, 2012, Chicago, IL, USA

DETC2012-71442

SIMULATION AND TESTING OF A 6-STORY STRUCTURE INCORPORATING A COUPLED TWO MASS NONLINEAR ENERGY SINK

Nicholas E. Wierschem
Dept. of Civil and Environmental Engineering
University of Illinois
Urbana, IL, USA

Jie Luo
Dept. of Civil and Environmental Engineering
University of Illinois
Urbana, IL, USA

Mohammad AL-Shudeifat
Dept. of Mechanical Science and Engineering
University of Illinois
Urbana, IL, USA

Sean Hubbard
Dept. of Aerospace Engineering
University of Illinois
Urbana, IL, USA

Richard Ott
Dept. of Mechanical Engineering
The University of Akron
Akron, OH, USA

Larry A. Fahnestock
Dept. of Civil and Environmental Engineering
University of Illinois
Urbana, IL, USA

D. Dane Quinn
Dept. of Mechanical Engineering
The University of Akron
Akron, OH, USA

D. Michael McFarland
Dept. of Aerospace Engineering
University of Illinois
Urbana, IL, USA

B. F. Spencer Jr.
Dept. of Civil and Environmental Engineering
University of Illinois
Urbana, IL, USA

Alexander Vakakis
Dept. of Mechanical Science and Engineering
University of Illinois
Urbana, IL, USA

Lawrence A. Bergman
Dept. of Aerospace Engineering
University of Illinois
Urbana, IL, USA

ABSTRACT

The nonlinear energy sink (NES) is a passive device used to rapidly direct energy into higher modes of vibration and locally dissipate a significant portion of the impulsive shock energy induced in the primary, linear structure to which it is attached. The Type III NES is a two degree-of-freedom device comprised of two lightweight masses coupled together through an essentially nonlinear element. The lower mass in this two-mass arrangement is coupled to the linear structure through another essentially nonlinear element. This modification has been found to dramatically improve the performance of the NES to mitigate the shock when compared to a one degree-of-freedom NES device. The measure of effective damping of the linear structure indicates the ability of the NES to dissipate energy and reduce the response of the structure across a wide range of energies. Experimental tests have been performed to verify the numerical findings. Good agreement between numerical predictions and experimental observations validates the identified model of the NES.

INTRODUCTION

In recent years nonlinear energy sinks (NESs) have been studied as supplemental damping devices to help mitigate vibrations in mechanical and structural systems. In its simplest form, also known as a Type I NES, a NES consists of a mass connected to the underlying system with a viscous damping element and an essentially nonlinear spring element. This essential nonlinearity means the NES has no linear stiffness component, thus no preferred vibration frequency. This allows the NES to vibrate with any mode of the structure and

participate in Targeted Energy Transfer (TET) [1], the transfer of energy from lower modes of vibration to higher ones where it is can be dissipated faster. Additionally, energy transferred to the NES itself is dissipated through damping in the NES.

Thus far, the majority of the work studying NESs has been analytical or numerical and relatively few experimental studies have been published. The experimental studies that have been conducted mostly utilize relatively small table top size specimens [2] [3] [4] [5] and some medium-scale specimens [6]. Additionally, even though numerical results have shown the effectiveness of the Type III NES [6], very few experimental studies have considered the Type III NES [7], which consists of two Type I NESs in series.

This study explores the response of a large-scale base structure with a Type III NES attached when subjected to an impulse-like ground motion. The NES utilizes specially shaped elastomeric bumpers as its nonlinear spring element and its dynamic properties are experimentally identified. These experimental results are then compared to numerical simulations.

NES AND BASE STRUCTURE

The linear base structure, which the NES considered for the experiments in this study is attached to, is a six-story structure found in the Smart Structures Technology Laboratory at the University of Illinois, see Figure 1. This 970 kg structure is 1.97 m tall and consists of 711 mm x 1143 mm x 25 mm steel floor plates supported by 6 steel columns. The use of high strength steel in the columns allows the structure to undergo substantial deformations without yielding the columns. In the experimental work in this study, the structure is loaded along its weak axis. In this direction the natural frequencies of the base structure, not considering the mass of the NES, are 1.62, 4.51, 7.46, 9.78, 11.65, and 14.43 Hz. Although the center of mass and stiffness of the structure are nearly collinear with the loading, small imperfections allow the torsional modes of the structure to be excited; the relevant torsional natural frequencies of the structure are 2.93, 12.77, 17.27, and 20.63 Hz. This structure is attached to a shake table, which is used to excite the structure with a step-function like ground motion meant to simulate an impulsive load. During the experiments, accelerations are recorded at each level via uniaxial capacitive accelerometers.

Figure 1: 6 Story Base Structure with NES attached

The NES used in this study is attached to the top floor of the linear base structure. This NES, which is shown attached to the top floor plate of the base structure in Figure 2, is a Type III NES, which is a two-mass NES where the masses are connected in series by nonlinear spring elements. In this implementation, the second (top) mass is nested within the first (bottom) mass. The masses of the top and bottom NES stages are 21 and 28 kg, respectively, which corresponds to 2.2 and 2.9% of the total mass of the structure, respectively. The bottom NES mass is mounted on a set of bushing bearings and can move along round rails that are connected to the linear base structure. The top NES mass is mounted on cart that moves along a rail connected to the bottom NES mass. The nonlinear spring forces that link the top floor of the linear base structure to the bottom NES mass and the bottom NES mass to the top NES mass are provided by elastomeric bumpers attached to the NES. Attention is paid when placing the elastomeric bumpers to ensure the bumpers are not initially compressed or there is any gap in which the NES is not in contact with either bumper. These elastomeric bumpers are replaceable and can be shaped to utilized geometric nonlinearities in combination with material properties to provide a desired nonlinear restoring force in an elastic and highly repeatable manner. Additionally, both stages of the NES can be locked so that the response of the base structure without the NES can be examined without considering added mass effects.

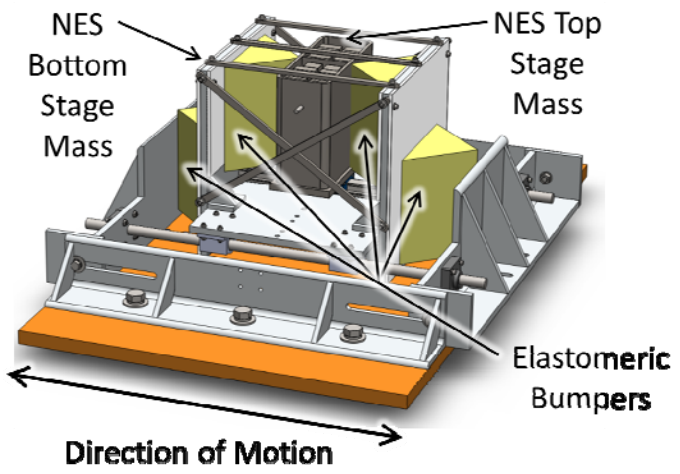

Figure 2: Rendering of Type III NES attached to top floor of test structure

EFFECTIVE MEASURES

To evaluate the performance of the NES in regards to reducing the response of the base structure, a set of measures is needed; however, due to the nonlinear response of the structure, typical linear measures, such as damping ratio, do not directly apply. As a consequence of this, a measure, referred to as effective damping, was developed to take into account both the energy dissipation and transfer provided by the NES [8]. The calculation of this effective damping is done first by converting the resulting response of the base structure due to the ground motion into modal coordinates. In terms of modal coordinate, q, the mass normalized single-degree-of-freedom (SDOF) equation of motion (EOM) for each mode is:

$$\ddot{q} + \lambda_{eff}\dot{q} + \omega_{eff}^2 q = 0 \tag{1.1}$$

In this equation, λ_{eff} is the instantaneous effective damping, and ω_{eff} is the instantaneous effective modal stiffness. The average effective damping, $\bar{\lambda}_{eff}$, can be derived by multiplying the EOM by $\dot{q}$ and integrating over the length of the record.

$$\int_{T_0}^{T_{end}} \dot{q}\ddot{q}dt + \int_{T_0}^{T_{end}} \dot{q}\lambda_{eff}\dot{q}dt + \int_{T_0}^{T_{end}} \dot{q}\omega_{eff}^2 q dt = 0 \tag{1.2}$$

The result of this integration is:

$$\begin{aligned}\frac{1}{2}\dot{q}^2(T_{end}) - \frac{1}{2}\dot{q}^2(T_0) + \bar{\lambda}_{eff}\int_{T_0}^{T_{end}} \dot{q}^2 dt \\ + \frac{1}{2}\bar{\omega}_{eff}^2 q^2(T_{end}) - \frac{1}{2}\bar{\omega}_{eff}^2 q^2(T_0)\end{aligned} = 0 \tag{1.3}$$

Assuming that the changes in effective stiffness are small, this equation can be simplified by replacing the average effective modal stiffness, $\bar{\omega}_{eff}$, with ω_n, the natural frequency of the mode. This expression can be solved for the average effective modal damping as follows:

$$\bar{\lambda}_{eff} = \frac{\left(\begin{array}{c}\frac{1}{2}\dot{q}_i^2(T_0) - \frac{1}{2}\dot{q}_i^2(T_{end}) + \\ \frac{1}{2}\omega_n^2 q_i^2(T_0) - \frac{1}{2}\omega_n^2 q_i^2(T_{end})\end{array}\right)}{\int_{T_0}^{T_{end}} \dot{q}_i^2 dt} \tag{1.4}$$

NONLINEAR SYSTEM IDENTIFICATION

As mentioned in the previous section, the elastomeric bumpers used to provide the nonlinear NES restoring force can be shaped to obtain a desired restoring force profile. In this work, an optimization study was used to determine the coefficients of the nonlinear stiffness terms, assuming cubic stiffness, to maximize the effective damping in the 1st mode of the base structure when subjected to a design loading. With this desired restoring force profile as the target for the top and bottom NES stages, elastomeric bumper were manufactured to replicate the optimal parameters. To experimentally confirm the properties of the NES, a nonlinear system identification was perform. The technique used for this experimental identification is the restoring force surface method [9]. This method is based on the equation of motion for the system. For example, because the top NES does not have any external forces directly applied to it during a ground motion, the equation of motion for this mass is:

$$\begin{aligned}m_{TopNES}\ddot{x}_{TopNES} + \\ f_R\left(\dot{x}_{TopNES}, x_{TopNES}, \dot{x}_{BotNES}, x_{BotNES}\right)\end{aligned} = 0 \tag{1.5}$$

Where m_{TopNES} is the known mass of the top NES, $\ddot{x}_{TopNES}$ is the absolute acceleration of the top NES mass, and f_R is generic restoring force term. For the top NES mass, the restoring force is a function of $\dot{x}_{TopNES}$, x_{TopNES}, $\dot{x}_{BotNES}$, and x_{BotNES} (the velocity and displacement of the top and bottom NES masses can be estimated from experimentally collected accelerations). Due to the knowledge of the top NES mass and

acceleration record, the generalized restoring force time history is known as well.

$$f_R\left(\begin{matrix}\dot{x}_{TopNES}, x_{TopNES},\\ \dot{x}_{BotNES}, x_{BotNES}\end{matrix}\right) = -m_{TopNES}\ddot{x}_{TopNES} \qquad (1.6)$$

This known generalized restoring force can then be set equal to an assumed form for the restoring force. In the case of the top NES mass, this assumed form consists of a viscous damping term, a linear stiffness term, and a nonlinear stiffness term

$$f_R = \begin{matrix} c\left(\dot{x}_{TopNES} - \dot{x}_{BotNES}\right) + k\left(x_{TopNES} - x_{BotNES}\right) + \\ k_{nl}\,\mathrm{sgn}\left(x_{TopNES} - x_{BotNES}\right)\left|x_{TopNES} - x_{BotNES}\right|^{\alpha} \end{matrix} \qquad (1.7)$$

Where c is the viscous damping coefficient, k is the linear stiffness coefficient, k_{nl} is the nonlinear stiffness coefficient, and α is the order of the nonlinear stiffness term. With the known restoring force and estimated displacements and velocities these parameters can be fit to complete the identification of the system top NES mass. A similar procedure is used to identify the system parameters of the bottom NES mass; however, in this case it is slightly more complicated due to the connection to both the top floor of the structure and the top NES mass.

The results of the identification of the NES are summarized in Table 1. In Figure 3 and Figure 4 the identified model of the restoring force from the stiffness components of the top and bottom NES stages are compared to the NES stiffness model from the optimization study over the range of relative displacements measured. These figures show that for each stage of the NES, even though the exponent of the nonlinearity is higher than exponent used in the optimization analysis, the combination of the nonlinear and the weak linear parts of the stiffness produce an experimentally identified model that provides a reasonable fit to the calculated optimal stiffness profile over the range of displacements consider.

	Top NES	*Bottom NES*
c $\left(N\text{-}s/m\right)$	132	96.3
k $\left(N/m\right)$	3302	1647
k_{nl} $\left(N/m^{\alpha}\right)$	3.50E+11	1.07E+12
α	6.03	6.13

Table 1: Identified NES parameters

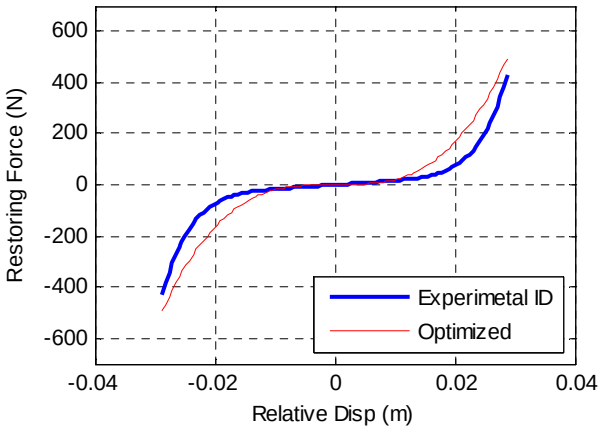

Figure 3: Comparison between restoring force from optimized stiffness and identified stiffness model for top NES

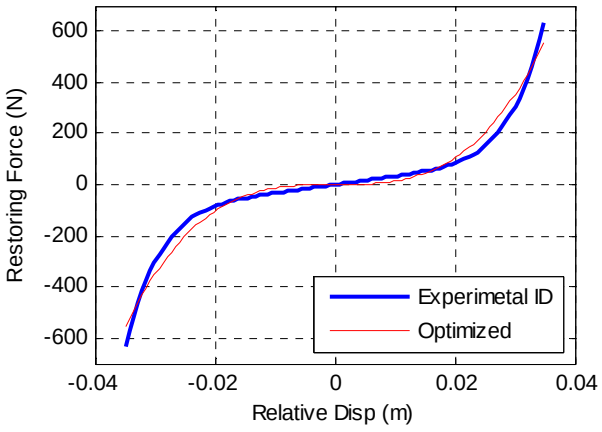

Figure 4: Comparison between restoring force from optimized stiffness and identified stiffness model for bottom NES

EXPERIMENTAL RESULTS

In the experiments presented in this study, the base structure is excited via a shake table with a short impulse-like ground motion of varying amplitude. An example of this ground motion is shown in Figure 5.

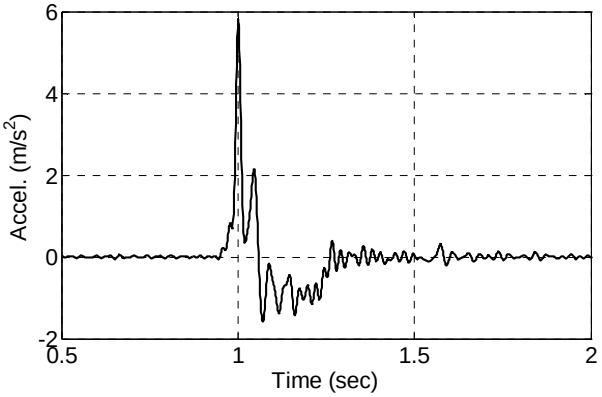

Figure 5: Ground acceleration record produced by shake table

When subjected to the specific ground motion seen in Figure 5, the top floor acceleration of the base structure with the NES locked and unlocked is shown in Figure 6. This figure shows that when the NES is unlocked the response of the structure is decreased substantially in the first five seconds after the loading. In addition to showing a decrease in the amplitude of the acceleration response, Figure 6 also shows that, in the unlocked case, the response appears to be composed predominantly of high frequency accelerations, as opposed to the low frequency accelerations seen in the locked case. This can be examined in more depth by studying the wavelet of the top floor acceleration, which is shown in Figure 7. This figure does indeed show the phenomenon seen in the time history of the acceleration; when the NES is unlocked the response in the 1st mode of the structure is very quickly eliminated and energy in the response is transferred to the higher modes of the structure.

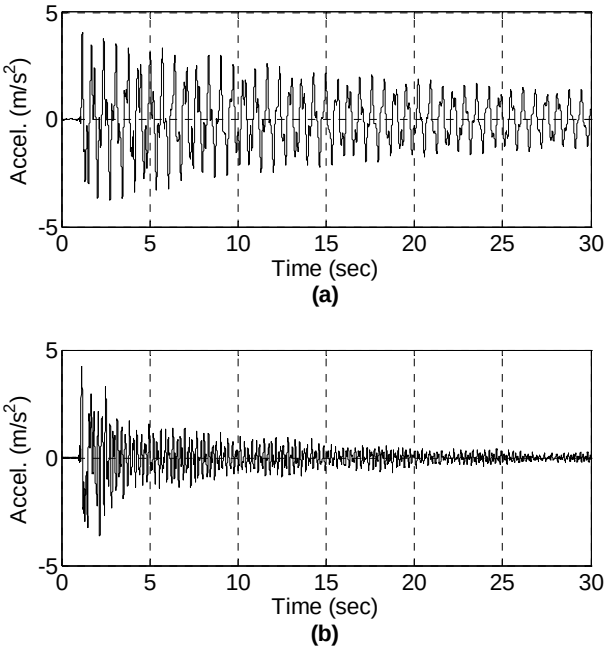

Figure 6: Top floor acceleration of the base structure with the NES a) locked b) unlocked

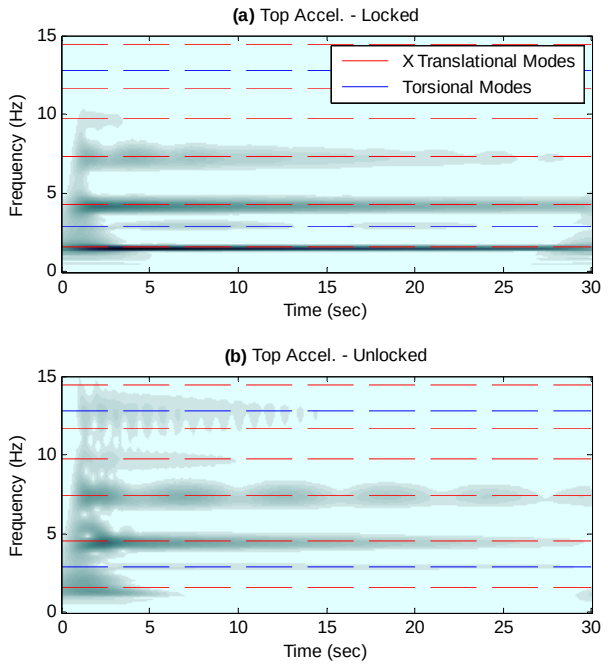

Figure 7: Wavelet of the base structure top floor acceleration with the NES a) locked b) unlocked

Figure 8 shows the displacement response of the top floor of the structure with the NES locked and unlocked, which is calculated from the measured acceleration record. This figure better serves to highlight the effect of the NES, as it shows that the NES is able to dramatically reduce the displacement of the structure within a very short time. Additionally, after this initial reduction in the response, the majority of the energy is in the higher modes of the structure, which further leads to a very small displacement.

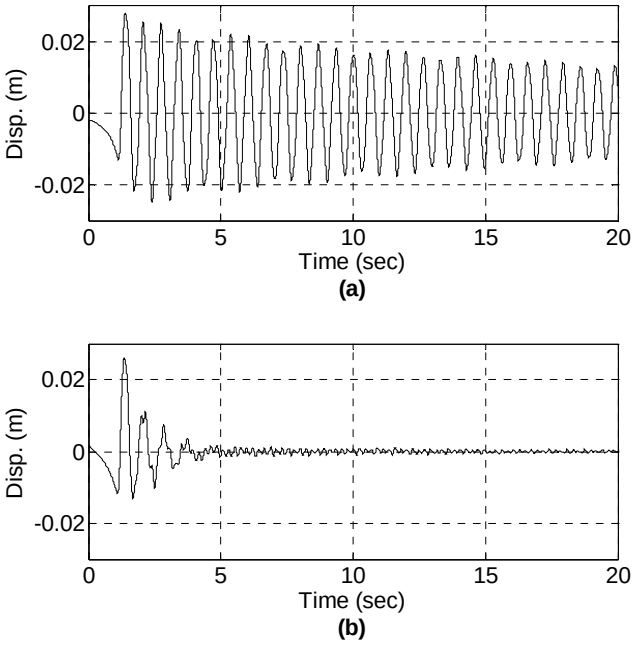

Figure 8: Top floor displacement of the base structure with the NES a) locked b) unlocked

Aside from assessing the effectiveness of the NES by comparing the time history or wavelet of the response, the effective damping measure that was introduced earlier is insightful. Figure 9 shows the resulting effective damping in the 1st mode of the structure across the range of ground motions studied. In this figure, each ground motion is identified by the total amount of calculated input energy to the system from the ground motion. Figure 9 shows that the effective damping provided by the NES to the 1st mode is much higher than the calculated effective damping of the system with the locked NES at all levels. Additionally one can see that effective damping is variable with the amount of input energy and that it peaks at a particular level. This peak level of effective damping occurs near the energy level that was used to determine the optimal NES parameters.

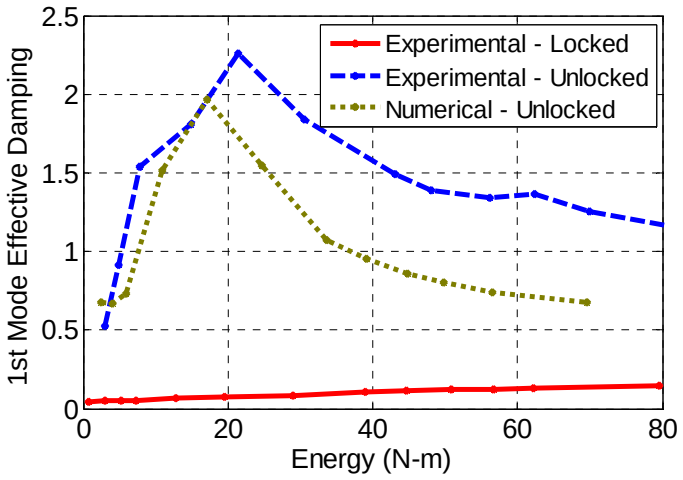

Figure 9: 1st Mode effective damping vs. input energy for experimental results with NES locked and unlocked and numerical results III NES

COMPARISON WITH NUMERICAL RESULTS

A numerical model of the system tested was created in MATLAB using the system identification results of the linear base structure and the nonlinear system identification results of the NES. This model considers 8 degrees-of-freedom (DOF), 6 translational DOF for each of the floors of the base structure in the direction of loading and 2 DOF for the NES; however, the model does not consider the DOF of the base structure related to translation perpendicular to loading or torsion. Figure 10 shows a mass, spring, damper representation of this simplified model.

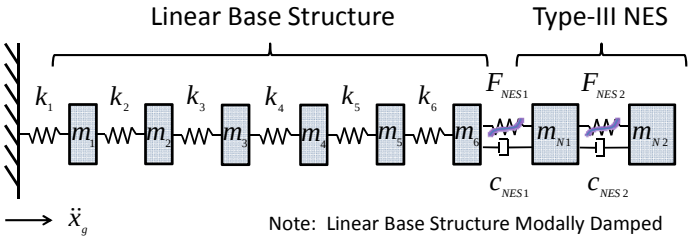

Figure 10: Representation of simplified model of base structure and NES system used in analysis

Using this model, numerical simulations of the system were performed with the experimentally recorded acceleration time histories from the base of the structure. For these numerical simulations the solver used in MATLAB was ODE45 and the relative tolerance was set to 1e-5, which was determined to be adequate to ensure accurate results. The resulting effective damping in the 1st mode of the structure for each of these simulations is shown in Figure 9 where it is compared with the experimentally determined effective damping value. As shown by this figure, the predicted

effective damping from the numerical model compares reasonably well with the experimentally determined value. Although the general shape is matched well, the numerical model modestly underestimates the magnitude of the effective damping, especially at high loads. Potential explanations for this include that at higher loads unmolded dynamics in of the NES, including any nonlinear damping from the bumpers, are more prevalent and the assumption of constant 1st mode stiffness used in the effective damping calculation is less realistic. In addition to comparing the performance of the numerical model with the experimental results by examining the effective damping measure, comparisons can be made using the time history results. In Figure 11 the top floor acceleration record is compared for the numerical simulation and experiment under the load level resulting in the peak effective damping measure. As shown in this figure the numerical simulation and experimental results show good agreement, with the primary noticeable differences appearing after the acceleration has been rapidly suppressed to a low level. These small differences are most likely due to unmodeled dynamics that are more prevalent at low amplitudes. Nevertheless, this good agreement in both time history results and global effective measures serves to verify the fidelity of the numerical model.

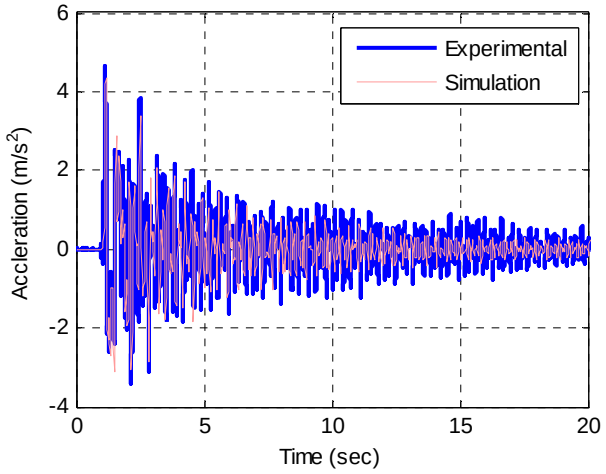

Figure 11: Top floor acceleration comparison between experimentally measured and numerical simulation

CONCLUSIONS

In this study the experimental testing of a two-stage nonlinear energy sink (NES) attached to a large-scale 6-story base structure is discussed. The NES used in this study is known as a type III NES and utilizes two masses connected in series with polyurethane bumpers to produce a nonlinear restoring force between the bottom NES mass and the top floor of the base structure and between the top and bottom NES masses. The restoring force profiles of the polyurethane bumpers, which were determined via an optimization study, are confirmed experimentally using the restoring force surface method. Experimental results for the base structure with NES attached show that the NES is capable of dramatically reducing the response of the structure to impulsive ground motion. This reduction in response is shown to be in part due to the NES transferring energy in the base structure from its low frequency modes to its high frequency modes, where it is dissipated in a shorter time frame. The experimentally measured effective damping in the 1st mode of the structure is shown to compare well with the numerical simulations, especially at energies at and before the peak in effective damping.

ACKNOWLEDGMENTS

This research program is sponsored by the Defense Advanced Research Projects Agency through grant HR0011–10–1–0077; Dr. Aaron Lazarus is the program manager. The content of this paper does not necessarily reflect the position or the policy of the Government, and no official endorsement should be inferred.

REFERENCES

[1] G. Kerschen, J. J. Kowtko, D. M. Mcfarland, L. A. Bergman, and A. F. Vakakis, “Theoretical and Experimental Study of Multimodal Targeted Energy Transfer in a System of Coupled Oscillators,” *Nonlinear Dyn*, vol. 47, no. 1–3, pp. 285–309, Aug. 2006.

[2] D. M. McFarland, G. Kerschen, J. J. Kowtko, Y. S. Lee, L. A. Bergman, and A. F. Vakakis, “Experimental investigation of targeted energy transfers in strongly and nonlinearly coupled oscillators,” *J. Acoust. Soc. Am.*, vol. 118, no. 2, pp. 791–799, 2005.

[3] E. Gourdon, N. A. Alexander, C. A. Taylor, C. H. Lamarque, and S. Pernot, “Nonlinear energy pumping under transient forcing with strongly nonlinear coupling: Theoretical and experimental results,” *Journal of sound and vibration*, vol. 300, no. 3–5, pp. 522–551, 2007.

[4] F. Nucera, F. Lo Iacono, D. M. McFarland, L. A. Bergman, and A. F. Vakakis, “Application of broadband nonlinear targeted energy transfers for seismic mitigation of a shear frame: experimental results,” *Journal of Sound and Vibration*, vol. 313, no. 1–2, pp. 57–76, 2008.

[5] E. Gourdon, C. H. Lamarque, and S. Pernot, “Contribution to efficiency of irreversible passive energy

pumping with a strong nonlinear attachment," *Nonlinear Dynamics*, vol. 50, no. 4, pp. 793–808, Feb. 2007.

[6] D. D. Quinn, S. A. Hubbard, N. E. Wierschem, M. A. Al-Shudeifat, R. J. Ott, J. Luo, B. F. Spencer, D. M. McFarland, A. F. Vakakis, and L. A. Bergman, "Equivalent modal damping, stiffening and energy exchanges in multi-degree-of-freedom systems with strongly nonlinear attachments," *Proceedings of the Institution of Mechanical Engineers, Part K: Journal of Multi-body Dynamics*, Jan. 2012.

[7] N. E. Wierschem, D. D. Quinn, S. A. Hubbard, M. A. Al-Shudeifat, D. M. McFarland, J. Luo, L. A. Fahnestock, B. F. Spencer Jr., A. F. Vakakis, and L. A. Bergman, "Passive Damping Enhancement of a Two-degree-of-freedom System Through a Strongly Nonlinear Two-degree-of-freedom Attachment," *Journal of Sound and Vibration*, submitted 2011.

[8] T. P. Sapsis, D. D. Quinn, A. F. Vakakis, and L. A. Bergman, "Effective Stiffening and Damping Enhancement of Structures With Strongly Nonlinear Local Attachments," *J. Vib. Acoust.*, vol. 134, no. 1, pp. 011016–12, Feb. 2012.

[9] K. Worden, "Data processing and experiment design for the restoring force surface method, part I: integration and differentiation of measured time data," *Mechanical Systems and Signal Processing*, vol. 4, no. 4, pp. 295–319, 1990.